S. Kadurin*, V. Kadurin

Odesa I. I. Mechnikov National University, Odesa, 65082, Ukraine

*Corresponding author: kadurins@gmail.com

The dynamics of Trooz Glacier, Antarctic Peninsula, by satellite remote sensing data

Abstract. The paper studies the ice cover of the Trooz Glacier, Kyiv Peninsula, West Antarctic Peninsula. The main goal of the work is to study the velocity dynamics of various parts of the Trooz Glacier in 2016−2022 based on remote sensing data and to compare them with changes in meteorological variables. The glacier's velocity was determined using 7-year data from the Copernicus Sentinel-1 satellite system based on the offset tracking technique. The characteristics of climatic changes during the same time intervals were determined according to the POWER project from NASA. To analyze the velocity field of the Trooz Glacier over time, 100 control points were selected along the entire valley from the mouth to the upland of the tributaries. For these points, values of the glacier velocity were calculated every 12 days for seven years, from 23.11.2015 to 28.12.2022. The entire glacier valley was divided into subclusters with their own average surface velocities and accelerations. To determine the level of climate change's influence on the velocities of different parts of the Trooz Glacier, we used the method of cross-correlation. The ice flow reacted to climatic changes with a certain delay. Annual velocity fluctuations of various parts and a slight glacier movement acceleration from 2015 to 2022 were identified. The latter amounted to 7−9% of the 2016-year speed. At the same time, only in the terminus area during the studied period was there a slight slowdown in the average annual velocity detected from 2.25 m day^{-1} in 2016 to 2.1 m day^{-1} in 2022. The most intensive climatic parameters affect the middle and lower parts of the Trooz Glacier. Among the main parameters, the near-surface environment temperature can be seen as the most influential force. Temperature changes impact the glacier velocity within the first 12 to 36 days; the effect can appear later with lag intervals of up to 120 days. The role of environmental temperature is significant for the middle part of the glacier, where its valley becomes wide. For the lower part and terminus region of the glacier, the temperature effect is most significant, with the reaction of the ice flow to temperature changes occurring in the coming days. Shortwave solar radiation and ultraviolet index were also established as influencers, but only for the lower and middle glacier parts, with a lag from 12 to 48 days. The influence of the precipitation amount was the most detectable only in the lower part of the glacier.

Keywords: glacier velocity, Kyiv Peninsula, offset tracking, Sentinel-1

1 Introduction

The melting Antarctic glaciers are a valuable source feeding the rising sea levels due to global climate change (The IMBIE team, 2018). Recent research has found that the Antarctic Peninsula presents one of the highest rates of movement and reces- sion of glaciers in Antarctica (Tuckett et al., 2019; Wallis et al., 2023). Almost all studies, not just the research on the mainland coastline, testify to a certain decrease in the ice cover. In particular, it was found for the Argentine Islands (Cook & Vaughan, 2010; Cook et al., 2014; Marusazh et al., 2019; Savchin & Shylo, 2020). In addition, the

glacial flows present a distinct seasonality (Zhou et al., 2014; Boxall et al., 2022; Wallis et al., 2023) related to the position and morphology of the glacial valley (Seehaus et al., 2018). Seehaus et al. (2015; 2018) also discovered short-term glacier flow fluctuations at the Antarctic Peninsula, which were attributed to a calving event and possible meltwater input. Thus, ice flow velocity here is largely influenced by the shape, size, and position of the glacier's valley on the one hand and the complex climatic conditions of the environment on the other hand. However, direct field observations of the flows are quite difficult due to the glacier's surface having a significant excess above sea level and the glacial flow extending far inland. In addition, there are no year-round stations on the Kyiv Peninsula in the study area, so it is extremely difficult to organize systematic studies of the Trooz Glacier's velocity.

In this case, in order to get and explore hard-to-reach areas in Antarctica, remote sensing (mostly satellite) data with a high spatiotemporal resolution have often been used (Jawak et al., 2018; Baumhoer et al., 2018; 2019). In general, the development of satellite observations is targeted to recognize objects (for example, to accurately map a coastline (Modava & Akbarizadeh, 2017)) and to establish their displacement and transformations in time (Nakamura et al., 2010). Copernicus Sentinel-1 satellite systems made it possible to obtain remote sensing data for various regions of Antarctica regardless of weather conditions and with sufficient temporal and spatial detail. This, in turn, made it possible to detect certain intra-seasonal (Zhou et al., 2011; Greene et al., 2018; Jawak et al., 2019; Tuckett et al., 2019; Boxall et al., 2022; Wallis et al., 2023;) and spatial variability (Nakamura et al., 2010) in the movement of glaciers.

Flow formation and the patterns of tension and fracturing are reflected in scientific research (De Rydt et al., 2019; Lhermitte et al., 2020; Surawy-Stepney et al., 2023a). However, the questions of the glacial flow's internal structure regarding displacement speed depending on the climatic conditions remain open. Therefore, the main

goal of this work is to establish relationships between the climatic characteristics of the environment and the velocities of different parts of the Trooz Glacier within the Kyiv Peninsula. The glacier was chosen because it is one of the largest glacial flows of the Antarctic Peninsula. Its flow is directed into the Penola Strait, almost opposite Galindez Island, where the Ukrainian Antarctic Akademik Vernadsky station is located. It exhibits the highest flow velocities in the lower part (Fig. 1).

2 Materials and methods
Satellite data processing
We use the data from the Sentinel-1 satellite for analysis. This satellite is equipped with a C-band-SAR device. It allows observing the Earth's surface in any weather, day and night. It has an active antenna with a radiation frequency of 5.405 GHz, which receives reflections from the Earth's surface in this wave range. In this way, an image of the Earth's surface, coastal strip, and ice sheets is formed, and the intensity of reflection from different types of surfaces is established. We used the first-level preprocessed images (Level-1) since they have an accurate spatiotemporal reference frame and contain information about the elevation marks of the surface, fitted to the Earth's ellipsoid (Ground Range Detected format data). The resolution of the datasets is 10 meters per pixel.

The images are publicly available on the Copernicus Open Access Hub https://scihub.copernicus.eu/dhus/#/home; the data are updated every 12 days. Therefore, we used images of the Trooz Glacier area from November 28, 2015, to December 28, 2022.

Sentinel-1 radar image data were processed via the Sentinel Application Platform (SNAP), freely available on the European Space Agency website https://step.esa.int/main/download/snap-download/.

We determined the velocity field for the Trooz Glacier using remote observations in the following way:

1. Matching and co-registering the images for different observation periods. The method is based on the fact that one of the two compared
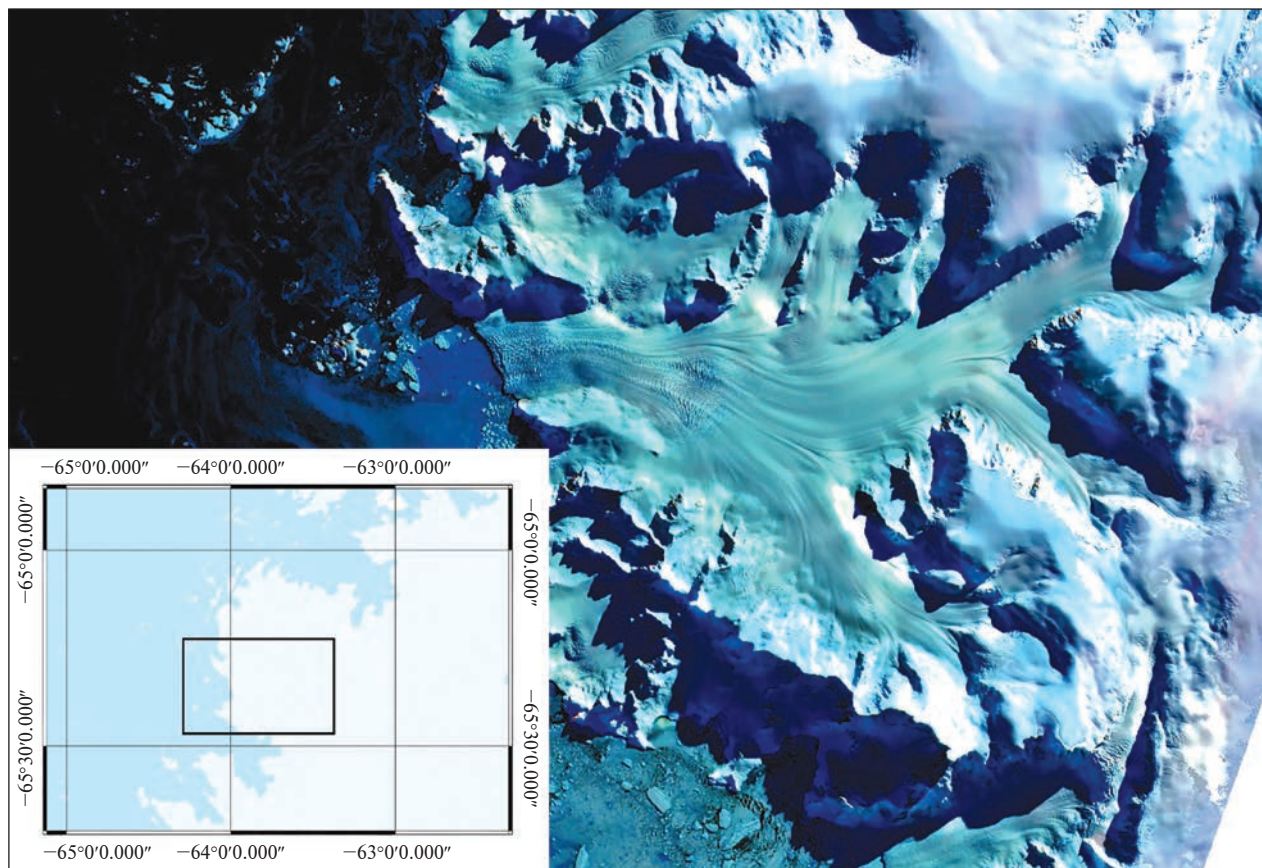
Figure 1. The position of the Trooz Glacier, Kyiv Peninsula, West Antarctic Peninsula. Satellite image based on the ESA Sentinel-2 from March 20, 2021, in RGB pseudo-colors — 11, 8A, 2 bands (https://scihub.copernicus.eu/dhus/#/home)

images is chosen as the main one and the other as the dependent one, and all its image pixels are adjusted to fit the coordinates of the main one. We used pairs of images with a minimum time interval of 12 days. This yielded 216 intervals for which changes in the ice cover were obtained, and ice flow velocities were calculated.

2. Definition of the study area. A full Sentinel-1 image covers 250×170 km of the Earth's surface; this contains a significant part of the Graham Coast, including a great extent of the ocean. The segment we needed for the study covers only 61×82 km. It shows the coastal part of the Kyiv Peninsula with the Trooz Glacier from its upland to the edge of Penola Strait.

3. Determining the glacier's velocity based on the displacements for different dates. This func-

tion is implemented as an Offset Tracking Operation software procedure for a pair of co-registered pictures with exact geo-positioning. It was designed specifically to track the glaciers. It has a certain sequence of actions, starting with reference point selection (without human input). These points must be present on both images and be precisely mapped. The program then calculates their spatial displacements. Since each image has precise geographic coordinates and timestamps, it is possible to calculate all of the reference points' velocities. Thirdly, the velocity field is presented as a digital surface. One reference point was selected for every 400×400 m plot, yielding 31.930 points for each pair of images. It makes it possible to determine the velocity field with sufficient detail and accuracy. That method is well-

known and widely spread for ice flow detection (Strozzi et al., 2002; Rignot et al., 2011).

4. Geo-positioning of the velocity field and its superimposition on the digital relief surface. This function includes determining the exact geographic reference for each selected point and correcting its elevation. This step compensates for the deviations due to the tilt of the satellite sensor and the specifics of the area's topography using the Doppler range orthorectification method. To adjust the elevation data, the program uses the state of the orbit, radar timing, and the inclination of the satellite sensor to the surface from the metadata for each remote image. In addition, it checks the findings against the digital surface of the relief. Elevation correction was based on the ACE30 GDEM digital surface for the research area. In addition, we used the positions of the nearest outcrops of crystal rocks to determine the accuracy of velocity calculations based on the offset tracking procedure. There are some big outcrops on the southern side of the lowest part of the valley close to the terminus. Based on these points, which do not move, we can determine the accuracy of the velocity interpolation model for each time interval.

In total, we obtained 216 velocity maps for the ice flow of the Trooz Glacier (see, e.g., in Fig. 2).

For all mapping purposes, ESA Copernicus Sentinel 2 images were used. One of the most uncloudy pictures of Trooz Glacier was taken on March 20, 2021. The false colour image with band 11 on the Red channel, band 8A on the Green channel, and band 2 on the Blue channel was generated for glacier structure detection.

Estimation of the speed of movement of the Trooz Glacier

The maps allowed us to estimate the general velocities and highlight particular areas with different values. Velocities of different parts of the ice flow could differ by almost an order of magnitude. Moreover, they changed depending on the season (Kadurin & Andrieieva, 2021). However, it is difficult to establish the exact velocities and

their changes over time for individual glacier parts. Instead, we selected a hundred reference points along the central flow lines of Trooz Glacier (Fig. 3).

Reference points are spread along the Trooz Glacier from its terminus to the main tributaries through the areas with the highest velocity numbers. The distance between the points varies from 500 m in the estuary to 1 km in the tributaries. This set-up allowed us to cover the entire massif of the glacier, even the tributaries, using only 100 points.

Thus, for each reference point, the glacier's velocity was determined for each of the 216 selected time intervals. The findings were analyzed and compared with the climate parameters observed during the same period.

Collection and analysis of climate data

Field climate observations in this area have certain limitations. Thus, the Akademik Vernadsky station is the closest point to the Trooz Glacier, where constant field measurements of climatic parameters are carried out. However, it is located on Galindez Island at a certain distance from the Antarctic Peninsula; the ocean and its currents strongly influence the results.

Therefore, we used the data from NASA's POWER project (https://power.larc.nasa.gov) to collect systematic information directly in the glacier area. This project includes information on long-term climate-averaged estimates of meteorological parameters and near-horizon solar fluxes obtained from NASA's Earth observation satellite systems (Table 1). This resource was created to obtain diverse, systematic, and accurate climate information for areas where conducting field observations is difficult or impossible. Data are provided as time series. Meteorological data based on simulations by the Modern Era Retrospective-Analysis for Research and Applications (MERRA-2) cover the time interval from 1981 to the present (Bosilovich et al., 2015). Solar radiation intensity data are based on remote observations using a set of channels measuring infrared radiation and their subsequent inversion to surface insolation within
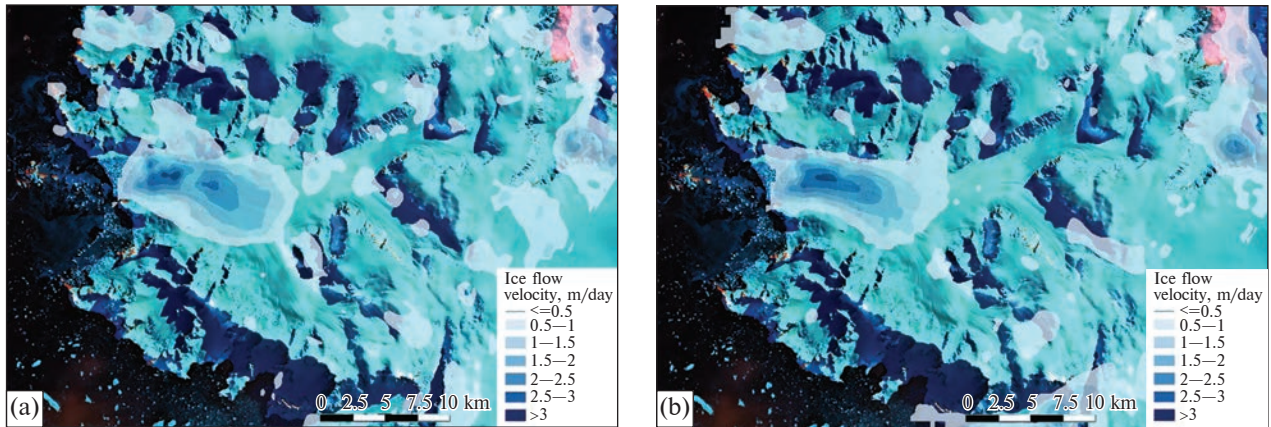
Figure 2. Velocity maps of the Trooz Glacier. (a) — January 1—13, 2020; (b) — August 30, 2022 — September 11, 2022. Based on the Sentinel-2 satellite image from March 20, 2021 in RGB pseudo-colours — 11, 8A, 2 bands (https://scihub.copernicus.eu/dhus/#/home)
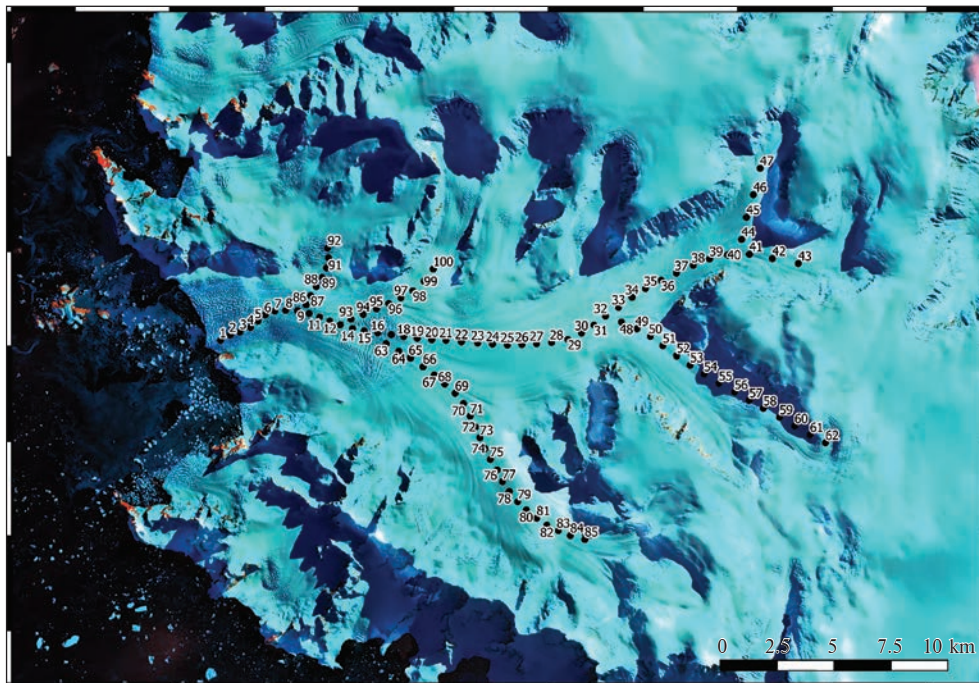

Figure 3. Points selected to trace the velocity of the Trooz Glacier. Based on the Sentinel-2 satellite image from March 20, 2021, in RGB pseudo-colors — 11, 8A, 2 bands (https://scihub.copernicus.eu/dhus/#/home)

the NASA CERES Fast Longwave and Short-wave Radiative project. The spatial resolution of these data is 1° in longitude and latitude for solar radiation and 0.5° in longitude and latitude for meteorological parameters.

The collected remote data were compared with the Akademik Vernadsky station field observations. It was found that NASA's POWER project remote data retain the general trend of changes in the main climatic parameters measured at the Aka-

demik Vernadsky station. The difference in temperature values shows that remote measurements above the glacier are always lower than field observations in the area of Galindez Island. At the same time, the amount of precipitation over the glacier is higher than recorded at the Akademik Vernadsky station. It should be noted that the presented remote data from NASA's POWER represent the total amount of precipitation without separating it by type. The accuracy of remote sensing methods for climate parameters measurements in Antarctica is discussed in an article (Gossart et al., 2019). Comparison of NASA MERRA-2 product data with other remote climate systems and ground-based observations showed that NASA MERRA-2 provides sufficient accuracy in determining climatic parameters in the Antarctic Peninsula and coastal areas.

We used the following parameters:

The spatial resolution of the climate model, which is 1° in longitude and latitude (Bosilovich et al., 2015), allows almost the entire area of the Trooz Glacier to be considered practically monotonous.

The exception is the near-mouth part of the glacier, where the meteorological parameters are no doubt under the influence of the ocean.

Statistical processing of the ice flow velocity data and their comparison with climatic parameters

The velocities of different parts of the glacier varied quite significantly. However, some patterns common to all observation points could also be identified to a first approximation. The velocity ranged from 4.1 ± 0.1 m day^{-1} to 0.1 ± 0.05 m day^{-1}. The highest velocity was determined for the points closest to the glacier's mouth. Another general feature was brief stages of acceleration of individual parts of the glacier followed by longer periods of slowed movement. Therefore, we used several statistical methods to analyse and compare data on the ice flow velocity at the selected points and on the climatic parameters from November 23, 2015, to December 28, 2022.

To begin with, the entire complex of points had to be grouped by their velocity changes in time. For this, we applied cluster analysis. This statis-

Table 1. NASA's POWER project climatic parameters detected for the Trooz Glacier area

| Code of climatic parameter	Description
ALLSKY_SFC_SW_DWN	Total shortwave radiation reaching the Earth's surface (kWh m^{-2} day^{-1})
ALLSKY_SFC_UV_INDEX	Total ultraviolet index, a dimensionless unit
T2M	Air temperature (°C) 2 meters above the ground
T2MDEW	Dew point/freezing point 2 meters above the ground (°C)
T2MWET	The "wet bulb" temperature 2 meters above the ground (°C)
TS	Temperature directly on the surface of the Earth, °C
T2M_RANGE	The difference between the maximum and minimum air temperatures 2 meters above the surface for the selected observation interval of 12 days, °C
T2M_MAX	Maximum air temperature 2 meters above the surface for the selected observation interval of 12 days, °C
T2M_MIN	Minimum air temperature 2 meters above the surface for the selected observation interval of 12 days, °C
QV2M	Average air humidity, g kg^{-1}
PRECTOTCORR	Adjusted total atmospheric precipitation for the observation interval of 12 days, mm
WS10M	Average wind speed 10 meters above the ground, m s^{-1}
WS10M_MAX	Maximum wind speed 10 meters above the ground for an interval of 12 days, m s^{-1}
WS10M_MIN	Minimum wind speed 10 meters above the ground for an interval of 12 days, m s^{-1}
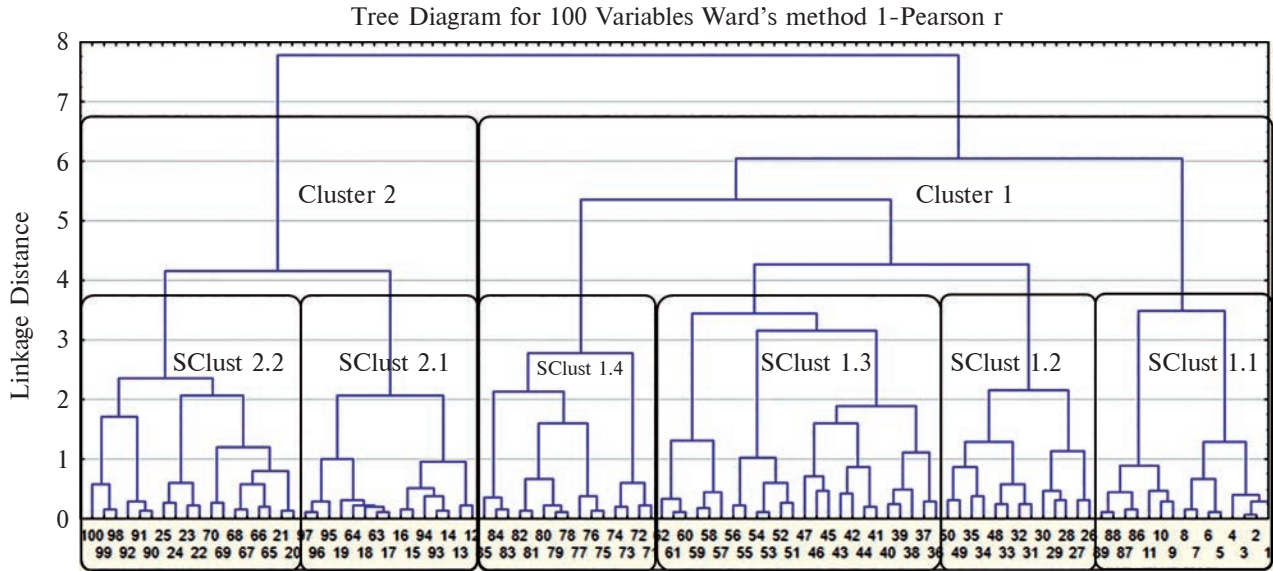
Figure 4. Diagram of the cluster analysis of the Trooz Glacier's selected points' distribution of velocity

tical method aims to classify an array of primary data and identify clusters based on similarity (in our case, by calculating Pearson correlation coefficients); all 100 points were pairwise compared in this way, and those with the largest correlation values were clustered together. Uniting individual variables into a single cluster and adding other variables were done after (Ward, 1963) by sorting with the minimization of the clusters' dispersion. Applying this method to the selected points' velocities made it possible to divide the entire glacier into segments and identify their main temporal movement patterns (Fig. 4).

The entire array of 100 points was divided into two main velocity Great Clusters. Each of these was, in turn, subdivided into separate subclusters

(four in the first, two in the second). Table 2 shows the numbers of the points included in each of the individual subclusters.

The presence of two main clusters indicates that the entire massif of the Trooz Glacier can be divided into two main parts according to the displacement velocity of the ice flow. In turn, each main part can be further divided into separate segments. Within each of these segments, specific local patterns of displacement can be established. Therefore, further comparison of the ice flow's velocity with the environment's climatic characteristics was done not for the individual points but for the subclusters (Fig. 5).

The slowness of the glacial masses and the possible delays in the environment's response to changes

Table 2. Points that formed large clusters and individual subclusters based on ice flow velocity

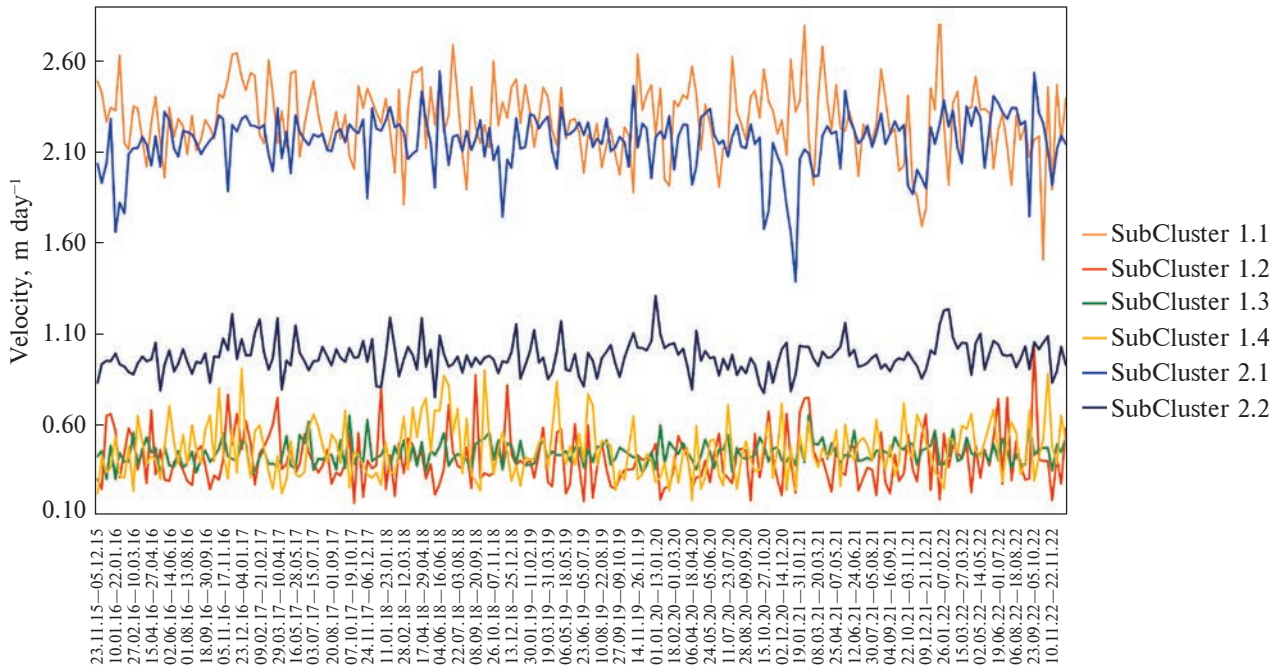| Cluster 1	Subcluster 1.1	1, 2, 3, 4, 5, 6, 7, 8, 9, 10, 11, 86, 87, 88, 89
	Subcluster 1.2	26, 27, 28, 29, 30, 31, 32, 33, 48, 34, 35, 49, 50
	Subcluster 1.3	36, 37, 38, 39, 40, 41, 44, 42, 43, 45, 46, 47, 51, 52, 53, 54, 55, 56, 57, 58, 59, 60, 61, 62
	Subcluster 1.4	71, 72, 73, 74, 75, 76, 77, 78, 79, 80, 81, 82, 83, 84, 85
Cluster 2	Subcluster 2.1	12, 13, 14, 93, 94, 15, 16, 17, 63, 18, 64, 19, 95, 96, 97
	Subcluster 2.2	20, 21, 65, 66, 67, 68, 69, 70, 22, 23, 24, 25, 90, 91, 92, 98, 99, 100

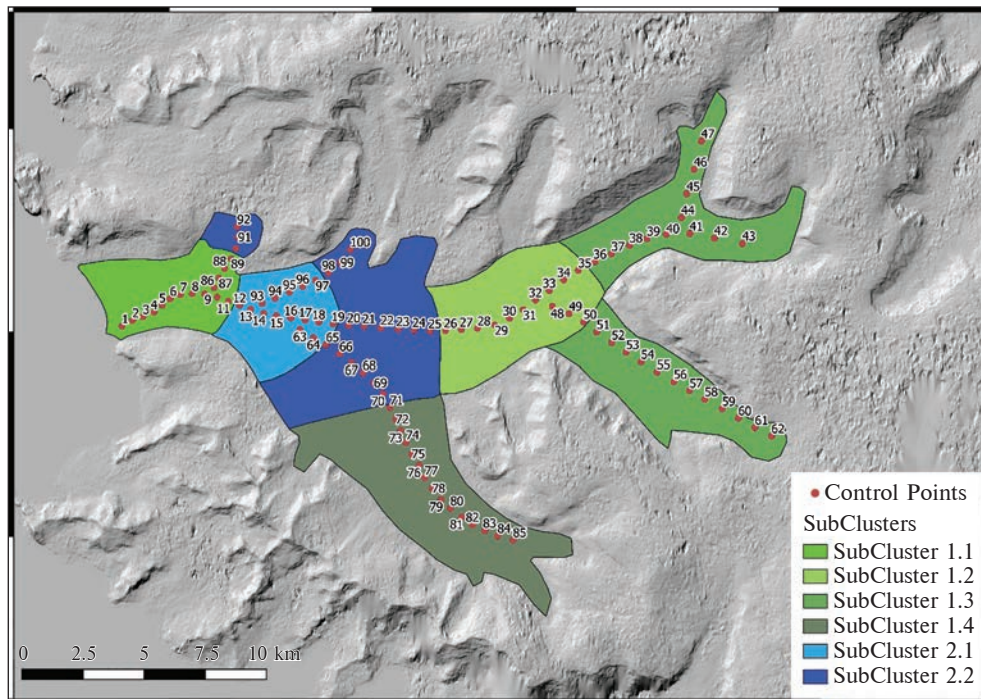**Figure 5.** Subclusters' velocity variations in 2015—2022

Figure 6. Spatial distribution of the detected subclusters of ice cover velocity based on an ASTER GDEM v3 Worldwide Elevation Data Model in shaded relief

in climatic parameters called for cross-correlation analysis (Derrick & Thomas, 2004). Under this method, the correlation coefficients are calculated as one data series is shifted stepwise relative to another. So, for each subcluster of the Trooz Glacier, the velocity data were averaged and then compared with climatic parameters so that, at first, the data series were matched exactly by date. The series of climatic data were shifted one step back so that velocity data were compared with the previous climate states. The shift allowed us to assess the relationship between data series with a delay of 12 days. The procedure was repeated; in total, 15 time periods were considered, which amounts to 180 days.

3 Results

Cluster analysis was used to divide the whole of Trooz Glacier into segments and find the main velocity parameters for each one (Fig. 6).

As a result, we found two large clusters which can be further divided into several subclusters. Great Cluster 1 encompasses the glacier's terminus area, tributaries, and the pre-glacial upland. Great Cluster 2 lies within the central part of the glacial valley. The subclusters have their own spatial patterns of position and velocity within the general trends. Attempts to tease out a periodical component using autocorrelation functions or the Fourier transform were unsuccessful.

Subcluster 1.1 covers the glacier's terminus. The velocities here are the greatest; the average velocity is 2.27 ± 0.2 m day^{-1}, and the maximum is 3.5 ± 0.21 m day^{-1}. This part is in immediate contact with the ocean. The whole ice thickness is crisscrossed by large fissures running in different directions. The velocity changes sporadically; decelerations directly follow accelerations. A comparison of the Trooz glacier velocity by SAR offset tracking and the NASA ITS_LIVE dataset (https://itslive-dashboard.labs.nsidc.org) showed the greatest difference in the terminus region. Speed values for ITS_LIVE are twice as high. At the same time, within the remaining parts of the glacier, the difference in speed is negligible. A similar situation with a significant deviation of the measured velocities by the SAR offset tracking method and NASA ITS_LIVE dataset for the terminus regions was encountered not only in our studies (Lee et al., 2023). Most likely, such a difference in the velocities of the lower part of the glaciers can be associated with the calculation algorithm used in ITS_LIVE or with grid spacing. In our studies, in the glacier speed calculation, the grid was 400 meters, and ITS_LIVE data was 240 m.

Subcluster 1.2 lies in an area bordered by high ledges with no substantial inflow within the main body of the glacier. The glacial matter here moves rather slowly, with insignificant oscillations from the average value of 0.4 ± 0.14 m day^{-1}. During all years, there were observed short-term (12−14 days long) periods of acceleration in the summer (from December to February). However, they followed no clear time or intensity pattern.

Subcluster 1.3 includes the upper parts of the main valley and tributaries that fall in that valley. The average velocity here is 0.44 ± 0.06 m day^{-1}, but a low increase in ice flow speed can be detected from 0.42 ± 0.06 m day^{-1} in 2016 to 0.46 ± 0.06 m day^{-1} in 2022 (Fig. 7).

Subcluster 1.4 covers the glacier's large southern tributary. That part differs from other glacier's inflows by a wide and flat valley. Surrounding slopes are quite gentle spatially from the southern part. These slopes are the source of a large amount of ice, which falls into the valley. As a result, the ice flow velocity here is slightly higher than other tributaries and somewhat increased from 0.45 ± 0.11 m day^{-1} in 2016 to 0.49 ± 0.10 m day^{-1} in 2022 (Fig. 7).

Subcluster 2.1 is situated near the glacier's terminus area. Like in the terminus area, all of the glacier is shattered by a series of crevasses. The average velocity here is 2.15 m day^{-1}. In addition, a general tendency to speed increase over time, which is typical for almost all subclusters, can be detected. The average velocity in 2016 was 2.1 ± 0.12 m day^{-1}, and in 2022, 2.22 ± 0.12 m × × day^{-1} (Fig. 7).
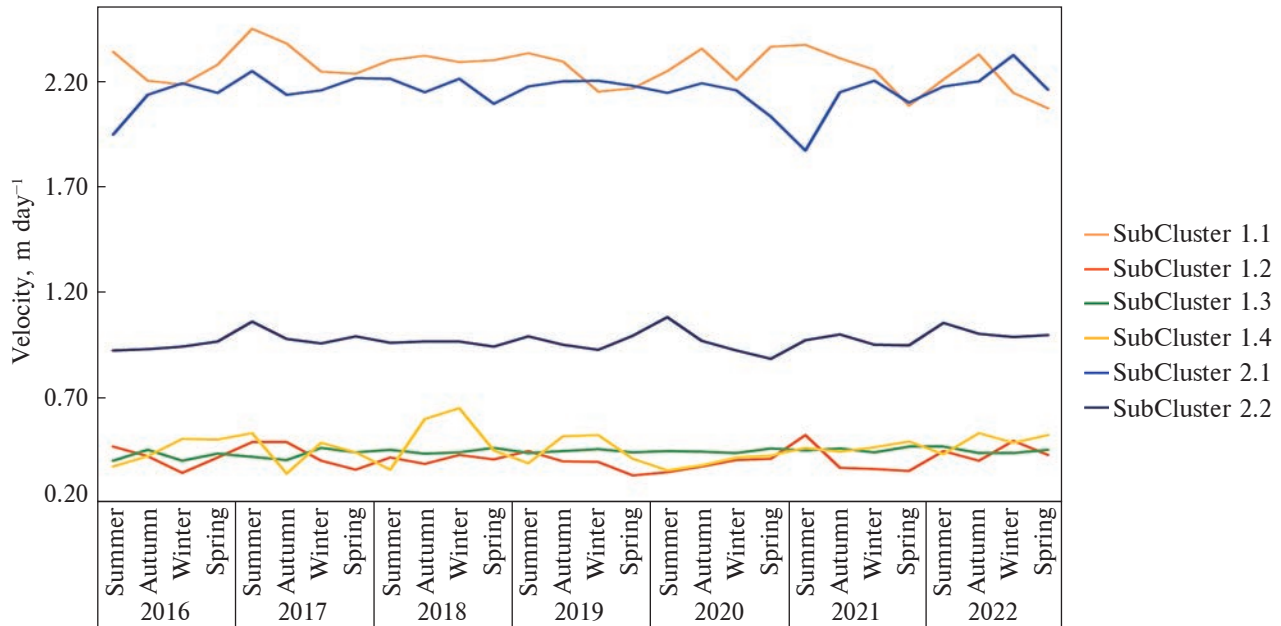
Figure 7. Subclusters' annual velocity variations

Subcluster 2.2 extends over the widest part of the glacier valley. Most of the tributaries fall into that part of the glacier. Here, the velocities of the ice flow are significant but not higher than 1.0 ± 0.07 m day^{-1} and also increased from 2016 to 2022. Unlike the previous subcluster, the surface here does not have many crevasses.

The Trooz Glacier's dynamics in 2016−2023 suggest a certain temporal pattern. The general distribution of various glacier subclusters' velocities indicates that the upper parts of the tributaries have an average speed of 0.4−0.45 m day^{-1}. In a place where all the flows of the glacier come together and form a single and wide valley, the speed will revert to up to 1 m day^{-1}. In the area of the terminus, the average speed increases to a maximum and, according to the results of remote observation, is 2.1−2.3 m day^{-1}, with short-term accelerations up to 3.5 ± 0.21 m day^{-1}. The lower, fastest part of the glacier is divided into two parts — subclusters 1.1 and 2.1. They have approximately the same average speeds but differ in general dynamics. Subcluster 1.1, adjacent to the ocean, has a weak deceleration trend over 2016−2022. Subcluster 2.1, like the main part of the glacier, has a slight tendency to increase in speed over the study period (Fig. 7). Such dynamics of the Trooz Glacier's various parts' movement can be caused by longer-period processes (Davies et al., 2012). To find out the reasons for such ice flow behavior, we compared the velocities of separate subclusters with the climatic parameters.

We obtained correlograms for the climatic parameters and the chosen subclusters of the glacier's velocity. The correlograms show the correlation coefficients of climatic parameters and the subclusters with a time lag of 0 to 15; each lag includes a 12-day interval. Correlograms also have a 95% confidence interval for the cross-correlation function. This statistic is calculated from the distribution parameters (mean and standard deviation) and allows to detect the anomalies. Since the cross-correlation is usually low, close to zero, the 95% confidence interval for almost all comparisons of climatic parameters and the subclusters' speed is in the range of 0.14÷−0.14. The values outside of the calculated interval can be considered statistically significant. Obtained cross-correlation values are quite low in absolute value and rather reflect the general possibility of a con-

nection between climatic parameters and velocities of different glacier parts.

The main correlational links between the velocities of the glacier's different parts and the climate parameters are as follows:

For the subcluster 1.1 (glacier's terminus), we detected cross-correlation connections with different climatic parameters. The intensity of solar radiation and ultraviolet radiation demonstrates a relationship with the speed of glacier movement in the terminus zone with a time lag of 3–6 (36 to 72 days). It is quite possible that increasing solar radiation intensity affects the temperature increase in the near-surface layer. At the same time, the same lag was detected between the reaction of that part of the glacier and air temperature, freezing point temperature, "wet bulb" temperature, maximum and minimum air temperatures, and temperature range. For the air temperature and the maximum air temperature, a connection with the glacier reaction was established with a lag of 0. It means the acceleration of the glacier movement in the terminus area occurs during the first 12 days after the rise of surface air temperature, and after that, another acceleration in this part of the glacier occurs with a delay of 3–5 lags (36–60 days).

On the other hand, the connection between the terminus subcluster's velocity and precipitation has lag 2 and a negative sign. Thus, decreasing precipitation leads to accelerating glacier flow but with a delay of 24 days. The common influence of temperature and precipitation on glacier velocity was discussed in different publications, not only for Antarctica (Davies et al., 2012; Lippl et al., 2019; Huang et al., 2023). Also, the influence of the near-surface wind speed on the speed of the glacier in the terminus was recorded with a lag 0, but with a negative value. That is, calm weather contributes to the acceleration of the glacier in the lower part almost immediately (in the first 12 days). The article (Van den Broeke & Van Lipzig, 2004) described the relationship between wind speed and surface temperature in Antarctica. That is probably the pattern we observed, with a de-

crease in wind speed leading to an increase in near-surface temperature, which in turn leads to the glacier's acceleration in the terminus zone.

Subcluster 1.2 presents cross-correlation with ultraviolet radiation with lag 2 (24 days) and with different temperature parameters — air temperature, freezing point temperature, "wet bulb" temperature, maximum and minimum air temperatures with lag 3 (36 days). In addition, negative cross-correlation was detected with wind speed with lag 4. Given that subcluster 1.2 is located in a narrow valley with steep slopes almost in the central part of the glacier, it can be assumed that there is a significant thickness of the ice flow. Several studies, including those done on the Antarctic Peninsula, indicate a similar structure of glaciers (Fretwell et al., 2013; Huss & Farinotti, 2014). In that case, a long delay between ice flow reaction and climatic influence is understandable.

Subcluster 1.3 correlates fairly weakly with environmental parameters. Only one cross-correlation parameter is detected — with wind speed with lag 8 (96 days). That subcluster covered the highest parts and tributaries of Trooz Glacier with bergschrund areas. A previous study (Osborn, 1983) shows that bergschrund zones have specific dynamics and active forces.

Subcluster 1.4 (upland of the large tributary in the glacier's south) presents a link with the intensity of solar radiation with lags from 0 to 3 and ultraviolet radiation with lags 2 and 3. Also, cross-correlation was detected between the velocity of that subcluster and air temperature, freezing point temperature, and "wet bulb" temperature with lags 0 and 10. At the same time, the correlation with lag 0 has a negative value. Connection with maximal air temperature appears at lag 10 and with minimal air temperature at lags 0 (negative value) and 13. The specificity of this subcluster is that it covers a wide tributary of the glacier, which faces from south to north. Thus, the surface energy balance will play a significant role for this part of the glacier and the lower parts where different tributaries come together. Short-wave solar radiation's role in glaciers' near-sur-

face temperature and melting has been the subject of many articles (Bintanja, 1995; Hoffman et al., 2008; Hofsteenge et al., 2022). In the example of that part of Trooz Glacier, we can find the negative correlation between the intensity of shortwave solar radiation and ultraviolet index with velocity with a small delay in reaction — from first to 36 days. Relations between solar energy income and near-surface temperature parameters here should account for ablation. However, in any case, the long-term delay connection (lag 10−13) with temperature parameters and glacier speed indicates that an increase in air temperature leads to the acceleration of a glacier's movements after a while.

Subcluster 2.1 covers the pre-terminus area of the glacier, and here, like in subcluster 1.4, we detected a connection with the intensity of solar radiation, ultraviolet index, air temperature, freezing point temperature, "wet bulb" temperature, maximum and minimum air temperature with lag 0 and negative value. A positive correlation between temperature parameters and ice velocity of that glacier part was also found, but with a time delay of lag 10 (120 days).

Subcluster 2.2 is the widest part of the glacier where all major tributaries meet. Its velocity is connected with several climate parameters. The statistically significant correlations start at lag 0 and appear at lag 2 for main temperature parameters. Therefore, a rise in temperature leads to the glacier's acceleration here practically at once, and this effect continues with a 24-day periodicity. Besides that, connections with the intensity of shortwave solar radiation and ultraviolet index at lags 4−5 (48−60 days) were established.

4 Discussion

The Trooz Glacier territory can be divided into three main parts according to velocity – upper, middle, and lower in the terminus area. Each has its specific velocity, movement dynamics, and relationship with environmental parameters.

The upper part includes two subclusters, 1.3 and 1.4. They both cover the bergschrund areas and the highest tributaries. They are characterized by relatively low velocity − about 0.45 m day^{-1}. However, the tributaries in subclusters 1.3 and 1.4 differ significantly in the ice flow dynamics and relationships with climatic parameters.

Subcluster 1.3, the most distant from the ocean coast, is located in narrow, deep valleys. Here, the glacier velocity varies insignificantly within a year, but there was a slight increase from 0.42 ± ± 0.06 m day^{-1} in 2016 to 0.46 ± 0.06 m day^{-1} in 2022. At the same time, no significant cross-correlations with climatic parameters were found here, except a relationship with wind speed with a lag 8 (96 days). Most likely, the process of formation and movement of the glacier is realized here without significant external climatic influences.

The area of subcluster 1.4 also covers a large tributary that originates from the bergschrund zone. We also recorded an increase in the average annual velocity from 0.45 ± 0.11 m day^{-1} in 2016 to 0.49 ± 0.1 m day^{-1} in 2022. However, this tributary has a wider valley than the other tributaries, is closer to the ocean, and has an orientation from south to north. As a result, the ice cover velocity varies significantly within the year. At the same time, the maximum velocities were detected in the Antarctic winter periods (June–August). Such an acceleration time for this part of the glacier explains the negative cross-correlations with temperature parameters and the amount of solar radiation at lag 0 and positive ones with the same parameters at lags 10−13 (120−156 days). In any case, it should be noted that the movement and velocity changes of the Trooz Glacier's upper tributaries are not closely connected with the studied climatic parameters.

The middle part of the glacier can also be divided into two parts — a narrow, deep valley (subcluster 1.2) and a wide part, formed when various tributaries join together (subcluster 2.2). Within the narrow valley, throughout the whole studied period, velocity of 0.4 m day^{-1} was detected. However, a cross-correlation with climatic parameters begins to appear more clearly here, among which temperature characteristics are of

primary importance. Several articles model glacier flow, the role of temperature, and the melt-water's participation in this process (Tuckett et al., 2019; Feldmann & Levermann, 2023). In our case, we recorded the speed increase in the central part of the glacier 36 days after the temperature rise. At the same time, for all parts of the glacier downstream to the terminus, the relationship with temperature parameters is preserved, and the delay becomes shorter. So, for the glacier's wider part, where all main valleys and tributaries come together (subcluster 2.2), there is also a correlation between the ice flow velocity and temperature parameters, but with a 12- to 36-day lag. The general tendency for almost the entire glacier to increase the average annual temperature from 0.96 m day^{-1} in 2016 to 1.01 m day^{-1} in 2022 is also preserved.

The lower part of the glacier also consists of two subclusters, 1.1 and 2.1. They differ from all other parts by the highest speed, 2.1−2.2 m day^{-1}. The glacier surface here is covered by a large number of crevasses. A relationship with temperature parameters with a lag 0 was also detected for this part. The glacier reaction occurs in the next 12 days after the change in environment temperature. At the same time, the correlation is positive for the terminus area, and negative for the pre-terminus. We also found a delayed reaction of the glacier's velocity to temperature parameters with a positive sign with a delay interval from 60 days for the terminus to 120 days for the pre-terminus. In addition to temperature, we established the influence of the intensity of solar radiation and the amount of precipitation for the glacier's lower part. Glacial crevasses' formation and movement are described in detail in a number of works (Zhao et al., 2022; Surawy-Stepney et al., 2023b). The role of 'crevasses' effect on the glacier movement mechanism is described in the work by Colgan et al. (2016). Based on these studies, the influence of solar radiation and other climatic parameters (such as surface air temperature and precipitation) on the velocity changes in the crevasse zone becomes clear.

5 Conclusions

The ice flow velocity within the Trooz Glacier increases from the upper tributaries to the terminus. So in the parts furthest away from the ocean, the glacier speed is on average 0.4−0.5 m day^{-1}; in the middle part, where the main flows converge, the average speed is about 1 m day^{-1}, and in the lower part and the terminus area, the average speed is 2.2−2.3 m day^{-1} with accelerations up to 3.5 m day^{-1}. Annual velocity fluctuations of various parts were identified, as well as a slight glacier movement acceleration from 2016 to 2022, which amounted to 7−9% of the 2016-year speed. At the same time, only in the terminus area, there was a slight decrease in the average annual velocity detected from 2.25 ± 0.2 m day^{-1} in 2016 to 2.1 ± 0.2 m day^{-1} in 2022.

The speeds of different parts of the Trooz Glacier and their general increase are influenced by climatic factors. However, the effect of climate on changes in the speed of glacier movement only occurs after a certain time delay. This type of relationship can be explained by the fact that a large mass and movement inertia characterize the glacial flow.

Climatic parameters most strongly affect the middle and lower parts of the Trooz Glacier. Among the main parameters, the near-surface environment temperature can be distinguished as the most influential force. Temperature impacts the glacier velocity within the first 12 to 36 days; the effect can appear later with a lag of up to 120 days. The relationship between the glacier's lower and middle parts' speed and intensity of shortwave solar radiation and the ultraviolet index was also established. The influence of these climatic parameters appears to have a more complex mechanism. Therefore, cross-correlation analysis shows that the glacier's response to the influence of these parameters was delayed by 12 to 48 days, depending on the glacier part. The influence of the atmospheric precipitation amount was the most pronounced only in the lower part of the glacier, where crevasses cover the entire surface.

Modern methods of remote observation of the glacier's speed make it possible to obtain systematic and operational information from Earth's surface areas where it is quite difficult to conduct field observations. The analysis of ice cover velocity determination for the Kyiv Peninsula and directly of the Trooz Glacier allows us to classify the study area and separate certain areas (clusters) according to the level of similarity in the dynamics of movements. Comparison of remote monitoring data of glacier's movement with the climatic environment characteristics made it possible to establish patterns of relationships between them. Climatic factors had the greatest influence on the lower and middle parts of the glacier. The dynamics of the upper tributaries in the bergschrund area are associated with the ice masses supplied from the plateau and weakly affected by climate change. The role of environmental temperature is significant from the middle part of the glacier, where its valley becomes wide. For the glacier's lower part and terminus, the temperature effect is most significant, with the reaction of the ice flow to temperature changes occurring in the coming days. Shortwave solar radiation and ultraviolet index were also established as influencers, but only for the lower and middle glacier parts, with a lag from 12 to 48 days. The influence of the atmospheric precipitation amount is most pronounced only in the lower part of the glacier.

References

Baumhoer, C. A., Dietz, A. J., Dech, S., & Kuenzer, C. (2018). Remote sensing of Antarctic glacier and ice-shelf front dynamics — A Review. *Remote Sensing*, *10*(9), 1445–1472. https://doi.org/10.3390/rs10091445

Baumhoer, C. A., Dietz, A. J., Kneisel, C., & Kuenzer, C. (2019). Automated extraction of Antarctic Glacier and Ice Shelf Fronts from Sentinel-1 imagery using deep learning. *Remote Sensing*, *11*(21), 2529. https://doi.org/10.3390/rs11212529

Bintanja, R. (1995). The local surface energy balance of the Ecology Glacier, King George Island, Antarctica: Measurements and modelling. *Antarctic Science*, *7*(3), 315–325. https://doi.org/10.1017/S0954102095000435

Bosilovich, M. G., Lucchesi, R., & Suarez, M. (2015). *MERRA-2: File Specification. GMAO Office Note No. 9 (Version 1.1)*. http://gmao.gsfc.nasa.gov/pubs/office_notes

Boxall, K., Christie, F. D. W., Willis, I. C., Wuite, J., & Nagler, T. (2022). Seasonal land-ice-flow variability in the Antarctic Peninsula. *The Cryosphere*, *16*, 3907–3932. https://doi.org/10.5194/tc-16-3907-2022

Colgan, W., Rajaram, H., Abdalati, W., McCutchan, C., Mottram, R., Moussavi, M. S., & Grigsby, S. (2016). Glacier crevasses: Observations, models, and mass balance implications. *Reviews of Geophysics*, *54*, 119–161. https://doi.org/10.1002/2015RG000504.

Cook, A. J., & Vaughan, D. G. (2010). Overview of areal changes of the ice shelves on the Antarctic Peninsula over the past 50 years. *The Cryosphere, 4*, 77–98. https://doi.org/10.5194/tc-4-77-2010

Cook, A. J., Vaughan, D. G., Luckman, A. J., & Murray, T. (2014). A new Antarctic Peninsula glacier basin inventory and observed area changes since the 1940s. *Antarctic Science, 26*, 614–624. https://doi.org/10.1017/S0954102014000200

Davies, B. J., Carrivick, J. L., Glasser, N. F., Hambrey, M. J., & Smellie, J. L. (2012). Variable glacier response to atmospheric warming, northern Antarctic Peninsula, 1988–2009. *The Cryosphere*, *6*, 1031–1048. https://doi.org/10.5194/tc-6-1031-2012

De Rydt, J., Gudmundsson, G. H., Nagler, T., & Wuite, J. (2019). Calving cycle of the Brunt Ice Shelf, Antarctica, driven by changes in ice shelf geometry. *The Cryosphere*, *13*, 2771–2787. https://doi.org/10.5194/tc-13-2771-2019

Derrick, T. R., & Thomas, J. M. (2004). Time-Series Analysis: The cross-correlation function. In N. Stergiou (Ed.), *Innovative Analyses of Human Movement* (pp. 189–205). Human Kinetics Publishers. https://dr.lib.iastate.edu/handle/20.500.12876/52528

Feldmann, J., & Levermann, A. (2023). Timescales of outlet-glacier flow with negligible basal friction: theory, observations and modeling, *The Cryosphere, 17*, 327–348. https://doi.org/10.5194/tc-17-327-2023.

Fretwell, P., Pritchard, H. D., Vaughan, D. G., Bamber, J. L., Barrand, N. E., Bell, R., Bianchi, C., Bingham, R. G., Blankenship, D. D., Casassa, G., Catania, G., Callens, D., Conway, H., Cook, A. J., Corr, H. F. J.,

Damaske, D., Damm, V., Ferraccioli, F., Forsberg, R., ... & Zirizzotti, A. (2013). Bedmap2: improved ice bed, surface and thickness datasets for Antarctica. *The Cryosphere, 7,* 375–393. https://doi.org/10.5194/tc-7-375-2013

Gossart, A., Helsen, S., Lenaerts, J. T. M., Broucke, S. V., van Lipzig, N. P. M., & Souverijns, N. (2019). An evaluation of surface climatology in State-of-the-Art Reanalyses over the Antarctic Ice Sheet. *Journal of Climate, 32*(20), 6899–6915. https://doi.org/10.1175/jcli-d-19-0030.1

Greene, C. A., Young, D. A., Gwyther, D. E., Galton-Fenzi, B. K., & Blankenship, D. D. (2018). Seasonal dynamics of Totten Ice Shelf controlled by sea ice buttressing. *The Cryosphere, 12,* 2869–2882. https://doi.org/10.5194/tc-12-2869-2018

Hoffman, M. J., Fountain, A. G., & Liston, G. E. (2008). Surface energy balance and melt thresholds over 11 years at Taylor Glacier, Antarctica. *Journal of Geophysical Research*, *113,* F04014. https://doi.org/10.1029/2008JF001029

Hofsteenge, M. G., Cullen, N. J., Reijmer, C. H., van den Broeke, M., Katurji, M., & Orwin, J. F. (2022). The surface energy balance during foehn events at Joyce Glacier, McMurdo Dry Valleys, Antarctica. *The Cryosphere*, *16,* 5041–5059. https://doi.org/10.5194/tc-16-5041-2022

Huang, D., Zhang, Z., Jiang, L., Zhang, R., Lu, Y., Shahtahmassebi, A., & Huang, X. (2023). Variability of glacier velocity and the influencing factors in the Muztag-Kongur Mountains, Eastern Pamir Plateau. *Remote Sensing, 15*, 620. https://doi.org/10.3390/rs15030620

Huss, M., & Farinotti, D. (2014). A high-resolution bedrock map for the Antarctic Peninsula. *The Cryosphere*, *8*, 1261–1273. https://doi.org/10.5194/tc-8-1261-2014

Jawak, S. D., Kumar, S., Luis, A. J., Pandit, P. H., Wankhede, S. F., & Anirudh, T. S. (2019). Seasonal comparison of velocity of the eastern tributary glaciers, Amery Ice Shelf, Antarctica, using SAR offset tracking. *ISPRS Annals of the Photogrammetry, Remote Sensing and Spatial Information Sciences*, IV-2/W5, 595–600. https://doi.org/10.5194/isprs-annals-IV-2-W5-595-2019

Jawak, S. D., Upadhya, A., Pandit, P. H., & Luis, A. J. (2018). Changes in velocity of Fisher Glacier, East Antarctica using pixel tracking method. *The International Archives of the Photogrammetry, Remote Sensing and Spatial Information Sciences*, XLII-5, 537–541. https://doi.org/10.5194/isprs-archives-XLII-5-537-2018

Kadurin, S., & Andrieieva, K. (2021). Ice sheet velocity tracking by Sentinel-1 satellite images at Graham Coast Kyiv Peninsula. *Ukrainian Antarctic Journal*, 1, 24–31. https://doi.org/10.33275/1727-7485.1.2021.663

Lee, S., Kim, S., An, H., & Han, H. (2023). Ice Velocity Variations of the Cook Ice Shelf, East Antarctica, from 2017 to 2022 from Sentinel-1 SAR time-series offset tracking. *Remote Sensing, 15*, 3079. https://doi.org/10.3390/rs15123079

Lhermitte, S., Sun, S., Shuman, C., Wouters, B., Pattyn, F., Wuite, J., Berthier, E., & Nagler, T. (2020). Damage accelerates ice shelf instability and mass loss in Amundsen Sea Embayment. *PNAS, 117*, 24735–24741. https://doi.org/10.1073/pnas.1912890117

Lippl, S., Friedl, P., Kittel, C., Marinsek, S., Seehaus, T. C., & Braun, M. H. (2019). Spatial and temporal variability of glacier surface velocities and outlet areas on James Ross Island, Northern Antarctic Peninsula. *Geosciences*, *9*, 374. https://doi.org/10.3390/geosciences9090374

Marusazh, Kh. I., Hlotov, V. M., & Siejka, Z. (2019). Monitoring of glacier frontal parts on Galindez and Winter islands (the Argentine Islands) in 2018–2019. *Ukrainian Antarctic Journal*, *2*(19), 26–37. https://doi.org/10.33275/1727-7485.2(19).2019.149

Modava, M., & Akbarizadeh, G. (2017). Coastline extraction from SAR images using spatial fuzzy clustering and the active contour method. *International Journal of Remote Sensing*, *38*(2), 355–370. https://doi.org/10.1080/01431161.2016.1266104

Nakamura, K., Doi, K., & Shibuya, K. (2010). Fluctuations in the flow velocity of the Antarctic Shirase Glacier over an 11-year period. *Polar Science*, *4*(3), 443–455. https://doi.org/10.1016/j.polar.2010.04.010

Osborn, G. (1983). Characteristics of the Bergschrund of an Avalanche-Cone Glacier in the Canadian Rocky Mountains. *Journal of Glaciology*, *29*(101), 55–69. https://doi.org/10.3189/S0022143000005141

Rignot, E., Mouginot, J., & Scheuchl, B. (2011). Ice Flow of the Antarctic Ice Sheet. *Science*, *333*, 1427–1430. https://doi.org/10.1126/science.1208336

Savchin, I., & Shylo, Ye. (2020). Monitoring of the ice caps area changes on Galindez, Winter and Skua Islands (Argentine Islands, West Antarctica). *Ukrainian Antarctic Journal*, 2, 42–49. https://doi.org/10.33275/1727-7485.2.2020.651 (In Ukrainian)

Seehaus, T., Cook, A. J., Silva, A. B., & Braun, M. (2018). Changes in glacier dynamics in the northern Antarctic Peninsula since 1985. *The Cryosphere*, *12*, 577–594. https://doi.org/10.5194/tc-12-577-2018

Seehaus, T., Marinsek, S., Helm, V., Skvarca, P., & Braun, M. (2015). Changes in ice dynamics, elevation and mass discharge of Dinsmoor-Bombardier-Edgeworth glacier system, Antarctic Peninsula. *Earth and Planetary Science Letters, 427,* 125–135. https://doi.org/10.1016/j.epsl.2015.06.047

Strozzi, T., Luckman, A., Murray, T., Wegmuller, U., & Werner, C. L. (2002). Glacier motion estimation using SAR offset-tracking procedures. *IEEE Transactions on Geoscience and Remote Sensing, 40*, 2384–2391. https://doi.org/10.1109/TGRS.2002.805079

Surawy-Stepney, T., Hogg, A. E., Cornford, S. L., & Davison, B. J. (2023a). Episodic dynamic change linked to damage on the Thwaites Glacier Ice Tongue. *Nature Geoscience, 16*, 37–43. https://doi.org/10.1038/s41561-022-01097-9

Surawy-Stepney, T., Hogg, A. E., Cornford, S. L., & Hogg, D. C. (2023b). Mapping Antarctic crevasses and their evolution with deep learning applied to satellite radar imagery. *The Cryosphere, 17*, 4421–4445. https://doi.org/10.5194/tc-17-4421-2023

The IMBIE team. (2018). Mass balance of the Antarctic Ice Sheet from 1992 to 2017. *Nature, 558*, 219–222. https://doi.org/10.1038/s41586-018-0179-y

Tuckett, P. A., Ely, J. C., Sole, A. J., Livingstone, S. J., Davison, B. J., van Wessem, J. M., & Howard, J. (2019). Rapid accelerations of Antarctic Peninsula outlet glaciers driven by surface melt. *Nature Communications, 10*, 4311. https://doi.org/10.1038/s41467-019-12039-2

Zhao, J., Liang, S., Li, X., Duan, Y., & Liang, L. (2022). Detection of surface crevasses over Antarctic ice shelves using SAR imagery and deep learning method. *Remote Sensing, 14*(3), 487. https://doi.org/10.3390/rs14030487

Zhou, C., Zhou, Y., Deng, F., AI, S., Wang, Z., & E, D. (2014). Seasonal and interannual ice velocity changes of Polar Record Glacier, East Antarctica. *Annals of Glaciology*, *55*(66), 45–51. https://doi.org/10.3189/2014AoG66A185

Zhou, C., Zhou, Yu., E, D., Wang, Z., & Sun, J. (2011). Estimation of ice flow velocity of calving glaciers using SAR interferometry and feature tracking. In *Proceedings of Fringe 2011 Workshop* (ESA SP-697). European Space Agency.

Van den Broeke, M., & van Lipzig, N. P. M. (2004). Changes in Antarctic temperature, wind and precipitation in response to the Antarctic Oscillation. *Annals of Glaciology*, *39*, 119–126. https://doi.org/10.3189/172756404781814654

Wallis, B. J., Hogg, A. E., van Wessem, J. M., Davison, B. J., & van den Broeke, M. R. (2023). Widespread seasonal speed-up of west Antarctic Peninsula glaciers from 2014 to 2021. *Nature Geoscience, 16,* 231–237. https://doi.org/10.1038/s41561-023-01131-4

Ward Jr., J. H. (1963). Hierarchical grouping to optimize an objective function. *Journal of the American Statistical Association*, *58*, 236–244. https://doi.org/10.1080/01621459.1963.10500845

С. Кадурін*, В. Кадурін

Одеський національний університет імені І. І. Мечникова,
м. Одеса, 65082, Україна

* Автор для кореспонденції: kadurins@gmail.com

**Динаміка льодовика Труз (Антарктичний півострів)
за даними супутникового дистанційного зондування**

Реферат. В статті представлено результати дослідження льодовика Труз в районі півострова Київ на західному узбережжі Антарктичного півострова. Метою було встановити динаміку швидкостей рухів його льодового покрову під впливом кліматичних чинників у 2016—2022-му роках за даними дистанційного спостереження та співставити її зі змінами метеорологічних чинників. Швидкості руху льодовика Труз визначалися за допомогою даних супутникової системи Copernicus Sentinel-1 на основі офсетного трекінгу. Характеристики кліматичних змін факторів за ті самі інтервали часу були визначені за даними спостережень проєкту POWER від NASA. Для аналізу поля швидкості льодовика Труз у часі було обрано 100 контрольних точок вздовж всієї долини, починаючи від гирла до верхів'їв приток. Для цих точок розраховувалися значення швидкості зміщення льодовика кожні 12 днів протягом трьох років. Це дозволило поділити всю долину льодовика на окремі кластери з притаманними тільки їм середніми значеннями швидкості та особливостями руху. Для встановлення рівня впливу змін кліматичних чинників на швидкість руху різних частин льодовика Труз був застосований крос-кореляційний метод порівняння, завдяки якому були виявлені реакції льодовикового потоку на зміни у кліматичних, і в першу чергу метеорологічних, параметрах середовища з певним запізненням у часі. Встановлені річні коливання параметрів для різних частин льодовика та деяке пришвидшення руху з 2016-го до 2022-го рр. (останнє сягало 7—9% швидкості, властивої 2016-му року). Лише в гирловій частині спостерігали певне зниження середньорічної швидкості з 2.25 м за добу (2016-й рік) до 2.1 м за добу (2022-й).

Найінтенсивніше кліматичні параметри впливають на середню та нижню частини льодовика Труз. Серед головних кліматичних параметрів приповерхнева температура є найвпливовішим фактором. Зміни температури впливають на швидкість льодовика протягом 12—36-и днів; вплив може проявитися і за 120 днів. Роль температури середовища важлива для середньої частини льодовика, де його долина стає широкою. Проте вплив температури найсильніший для нижньої і гирлової частин; льодовий потік реагує на зміни температури протягом кількох днів. В результаті дослідження встановлено вплив короткохвильового сонячного випромінювання та індексу ультрафіолета, але лише для нижньої та середньої частин льодовика, із затримкою в 12—48 днів. Вплив кількості опадів був показаний лише для нижньої частини льодовика.

Ключові слова: Sentinel-1, офсетний трекінг, півострів Київ, швидкість льодовика